Allosteric transitions of rabbit skeletal muscle lactate dehydrogenase induced by pH-dependent dissociation of the tetrameric enzyme

Allosteric transitions of rabbit skeletal muscle lactate dehydrogenase induced by pH-dependent dissociation of the tetrameric enzyme

Iacovino L.G.[1], Rossi M.[2], Di Stefano G.[3], Rossi V.[3], Binda C.[1], Brigotti M.[3], Tomaselli F.[2], Pasti A.P.[2], Dal Piaz F.[4], Cerini S.[5], Hochkoeppler A.[2,6]

[1]Department of Biology and Biotechnology, University of Pavia, Via Ferrata 1, 27100 Pavia, Italy

[2]Department of Pharmacy and Biotechnology, University of Bologna, Viale Risorgimento 4, 40136 Bologna, Italy

[3]Department of Experimental, Diagnostic and Specialty Medicine, University of Bologna, Via S. Giacomo 14, 40126, Bologna, Italy

[4]Department of Medicine, University of Salerno, Via Giovanni Paolo II 132, 84084 Fisciano, Italy

[5]Department of Industrial Chemistry "Toso Montanaro", University of Bologna, Viale Risorgimento 4, 40136, Bologna, Italy

[6]CSGI, University of Florence, Via della Lastruccia 3, 50019 Sesto Fiorentino, Firenze, Italy

Correspondence:

Alejandro Hochkoeppler
Department of Pharmacy and Biotechnology
University of Bologna
Viale Risorgimento 4
40136 Bologna
Italy
Phone: ++39 051 2093671
Fax: ++39 051 2093673
e-mail: a.hochkoeppler@unibo.it

Competing interests: none

ABSTRACT

Among the functions exerted by eukaryotic lactate dehydrogenases, it is of importance the generation of lactate in muscles subjected to fatigue or to limited oxygen availability, with both these conditions triggering a decrease of cellular pH. However, the mutual dependence between lactate dehydrogenase (LDH) catalytic action and lactic acidosis is far from being fully understood. Here we show that the tetrameric LDH from rabbit skeletal muscle undergoes allosteric transitions as a function of pH, i.e. the enzyme obeys Michaelis-Menten kinetics at neutral or slightly alkaline pH values, and features sigmoidal kinetics at pH 6.5 or lower. Remarkably, we also report that a significant dissociation of tetrameric rabbit LDH occurs under acidic conditions, with pyruvate/NAD^+ or citrate counteracting this effect. Moreover, citrate strongly activates rabbit LDH, inducing the enzyme to feature Michaelis-Menten kinetics. Further, using primary rabbit skeletal muscle cells we tested the generation of lactate as a function of pH, and we detected a parallel decrease of cytosolic pH and secretion of lactate. Overall, our observations indicate that lactic acidosis is antagonized by LDH dissociation, the occurrence of which is regulated by citrate and by allosteric transitions of the enzyme induced by pyruvate.

Key words: lactate dehydrogenase; rabbit muscle; pH-dependent allostery; Krebs cycle; citrate.

1. INTRODUCTION

Lactic acid represents an important metabolite, for both prokaryotic and eukaryotic organisms. Among prokaryotes, lactic acid bacteria constitute a group of microorganisms belonging to different genera, nevertheless sharing the competence in the generation of lactate as a fermentative end product [1]. This peculiar bacterial phenotype relies on lactate dehydrogenases (LDHs), responsible for the reduction of pyruvate to lactate according to a variety of mechanisms, exerted by NADH -dependent or -independent enzymes [2], yielding L- or D-lactate. Bacterial D-lactate dehydrogenases are homodimeric [3-5] or homotetrameric enzymes [6], featuring Michaelis-Menten [7] or cooperative kinetics [8]. Similarly, L-lactate dehydrogenases isolated from bacterial sources are homodimeric [9] or homotetrameric enzymes [2], with representatives featuring allosteric transitions and homotropic or heterotropic activation (e.g. by pyruvate and fructose 1,6-bisphosphate, respectively) [10]. Moreover, among bacterial allosteric enzymes the occurrence of low- and high-affinity quaternary structures was reported [10], with these alternative conformations corresponding to the T and R states defined by the classical Monod-Wyman-Changeux model [11].

Among eukaryotes, the presence of tetrameric L-LDHs in vertebrates was early detected [12], with D-LDHs thought to be exclusive of eukaryotic invertebrates [13]. However, it was quite recently recognized that genes coding for D-LDHs do occur in vertebrates [14], therefore suggesting that the two stereospecific forms of LDHs can be expressed in the same eukaryotic organism. Concerning the L-LDHs of vertebrates, two major isoforms were long ago identified, i.e. the heart (H, LDH-B) and the muscle (M, LDH-A) enzymes [15,16]. The H form is more abundant in aerobic tissues, and is supposed to mainly act in the oxidation of lactate. The M form is mainly produced in tissues facing

transient hypoxia, such as white muscle fibers, where it is devoted to the reduction of pyruvate. In addition, the X form (LDH-C) was isolated from mammalian spermatozoa [17], and it was detected in mitochondria [18].

Evolutionary speaking, it was shown that NADH-dependent L-lactate dehydrogenases originated from a LDH-like L-malate dehydrogenase ancestor, by means of two gene duplication events [19]. Recently, a detailed genomic analysis revealed the presence of a group of sequences coding for enzymes featuring intermediate properties between those of L-malate and L-lactate dehydrogenases [20]. Remarkably, peculiar catalytic properties were determined for a member of this group, i.e. the enzyme from *Tolumonas auensis*. In particular, this enzyme was shown to be competent in reducing oxaloacetate and pyruvate at the expense of NADPH, obeying Michaelis-Menten and sigmoidal kinetics, respectively [20].

Physiologically speaking, the relevance of lactate in energetic metabolism was long ago recognized [21], and it was also shown that muscles subjected to intense exercise face transient hypoxia which, in turn, leads to a net accumulation of lactate [22]. However, it has to be noted that lactate can be produced, albeit at moderate levels, in fully aerobic tissues [23,24], and it has been therefore proposed that lactate does always represent the end product of glycolysis [25]. According to this view, the cytosolic lactate produced under fully aerobic conditions is transferred to the mitochondrial intermembrane space, where it undergoes oxidation to pyruvate, which is finally committed to the Krebs cycle [25]. Therefore, any situation limiting the oxidative consumption of pyruvate (not necessarily oxygen limitation) would imply an increase of lactate level, a condition which is known to occur in cancer cells [26].

Under both physiological and pathological conditions, the occurrence of an energetic metabolism dominated by the glycolytic generation of lactate can be associated with a decrease of intracellular pH. It should be noted that the generation of lactate by LDH does not induce acidification *per se*,

the reduction of pyruvate at the expense of NADH + H^+ being a proton-consuming reaction. Lactic acidosis represents instead the outcome of a net release of H^+ from ATP hydrolysis under hypoxic or anoxic environments [27]. To extensively inspect lactic acidosis, different experimental conditions able to induce a significant drop in cytosolic pH were identified and analyzed. In particular, using KCN to inhibit the mitochondrial electron transfer chain (chemical hypoxia) the intracellular pH (pH_i) of cultured rat hepatocytes was observed to decrease down to 6.1 [28]. Further, the pH_i of rat astrocytes in animals subjected to ischemia was found to be strongly acidic, with extreme values determined below 6.0 [29]. Moreover, skeletal muscle cells from different animals were shown to feature pH_i values within the range 6.0-6.4 upon being exposed to hypoxic environment or to fatigue [30-32].

When considering skeletal muscle cells facing prolonged fatigue and hypoxia, the activity of LDH-A is essential for the energetic metabolism. However, the decrease in pH_i linked to hypoxic glycolysis and ATP consumption could trigger a parallel decrease in LDH-A activity, depressing in turn the energetic potential of lactate generation. We have recently shown that tetrameric human LDH-A undergoes consistent dissociation and features allosteric transitions when exposed to acidic solutions, with these pH-induced effects corresponding to low activity levels both *in vitro* and *in vivo* [33]. To investigate this point in further detail, we used rabbit skeletal muscle LDH (LDH-A) as a model system. Accordingly, we report here on the activity of rabbit LDH-A as a function of pH, and on the occurrence of cooperative kinetics under acidic pH conditions. In addition, the identification of rabbit LDH-A effectors and the characterization of enzyme stability over a wide pH interval are also presented, along with the determination of enzyme activity in rabbit skeletal muscle cells subjected to the acidification of cytosol.

2. MATERIALS AND METHODS

2.1 Materials

All reagents were purchased from Merck-Millipore (St. Louis, MO, USA).

2.2 Rabbit lactate dehydrogenase

Lactate dehydrogenase from rabbit skeletal muscle (LDH-A, enzyme suspension in 3.2 M ammonium sulfate) was obtained from Roche (Basel, Switzerland). LDH-A was dialyzed against 10 mM Tris-HCl (pH 7.5), concentrated to approximately 10 mg/mL with an Amicon ultrafiltration cell equipped with a YM100 membrane, and loaded onto a Superdex-200 gel filtration column (1.6 x 62 cm) previously equilibrated with 10 mM Tris-HCl (pH 7.5). Fractions (0.9 mL) eluted from the column and containing the tetrameric enzyme were pooled, concentrated, and aliquots of the concentrated enzyme solution were stored at -20 °C until used.

2.3 Recombinant lactate dehydrogenase

A synthetic gene, optimized for *Escherichia coli* codon usage and coding for rabbit LDH-A (Supplementary Information, Figure S1), was synthesized by GenScript (Leiden, NL). The gene accordingly obtained was cloned into the pET9a expression vector using the *NdeI* and *BamHI* restriction sites, yielding the pET9a-rbLDHA construct. Electro-competent *Escherichia coli* BL21(DE3) cells were transformed with pET9a-rbLDHA, and then selected using solid LB medium supplemented with kanamycin (40 μg/mL). To overexpress LDH-A, transformants were pre-cultured overnight in LB-kanamycin at 37 °C, under shaking (180 rpm). The pre-cultures were diluted (1:500) in fresh LB-kanamycin medium, cells were cultured for 9 h at 30 °C under shaking, and subsequently induced to overexpress LDH-A with 1 mM isopropyl-β-D-thiogalactopyranoside (IPTG). The induction was maintained for 15 h at 30 °C. Cells were then harvested, resuspended in buffer A (50 mM Tris-HCl,

50 mM NaCl, 5 mM EDTA, pH 7.5) supplemented with 1 mM phenylmethylsulfonyl fluoride (PMSF), and lysed by sonication (3 cycles of 2 min, 6 W). The crude protein extract accordingly obtained was centrifuged (15,000 x g, 20 min), the pellet was discarded, and the supernatant was immediately loaded onto a HiTrap Blue column (5 mL, GE Healthcare, Piscataway, USA), previously equilibrated with buffer A. After extensive washing of the column with buffer A, LDH-A was eluted with buffer A containing 0.5 M NaCl. The best fractions (as determined by activity assays and SDS-PAGE analysis) were pooled, and solid NaCl was added to increase its concentration to 3.5 M in the pooled fractions. The sample accordingly obtained was loaded onto a HiTrap Phenyl FF column, previously equilibrated with Buffer A containing 3.5 M NaCl. After washing the column, a reverse NaCl gradient (3.5-1.0 M) was applied (10 column volumes), and afterwards LDH-A was eluted with buffer A containing 1 M NaCl. The best eluted fractions were pooled, concentrated to 2 mL and loaded onto a Superdex-200 column, equilibrated with 10 mM Tris-HCl, pH 7.5. After pooling and concentrating the fractions containing homogeneous tetrameric LDH-A, aliquots of the concentrated purified enzyme were stored at -20 °C until used.

2.4 Activity assays

The enzyme-catalyzed reduction of pyruvate was assayed by determining the decrease in Absorbance at 340 nm related to the oxidation of β-NADH. The extinction coefficient of β-NADH at 340 nm was assumed equal to $6.22 \bullet 10^3$ M^{-1} cm^{-1} [34]. The oxidation of lactate in the presence of NAD^+ was similarly assayed at 340 nm. All the assays were performed in duplicate at 25 °C, using a Cary 300 Bio spectrophotometer and starting reactions by enzyme addition. To analyze enzyme kinetics as a function of pH, a universal buffer (containing Mes, Mops, and Tris, 25 mM each) was used [35]. The enzyme kinetic parameters were determined with the Levenberg-Marquardt algorithm in SigmaPlot 14 (Systat Software, San Josè, CA, USA), using the mean of the two values of initial reaction velocity independently determined at each substrate concentration. In particular,

the parameter $K_{0.5}$ refers to the substrate concentration corresponding to half-maximal reaction velocity under conditions of cooperative kinetics. The Protein concentration was assayed according to Bradford [36].

To assess the effect, if any, triggered by the intermediates of Krebs cycle on LDH-A activity, stock solutions of each compound to be tested were prepared in distilled H_2O supplemented with the appropriate volume of NaOH to obtain pH 5.0. The pH of each stock solution accordingly prepared was checked with litmus paper. An identical procedure was used to prepare stock solutions at pH 5.0 of glutamate, aspartate, glutarate, and acetate. Particular care was taken with oxaloacetate (known to be unstable), the stock solutions of which were prepared immediately before use.

2.5 Crystallization, data acquisition, and structure determination

L-lactate dehydrogenase from rabbit skeletal muscle (Roche) was gel-filtered on a Superdex 200 10/300 column conditioned with 40 mM Hepes buffer (pH 7.5). Fractions were pooled and concentrated using a Amicon Ultra-4 Centrifugal Filter Unit with Ultracel-30 membrane. The final enzyme concentration was adjusted to 5 mg mL^{-1}. Crystals were grown using the hanging drop vapour diffusion method at 20 °C in a solution containing 8-13% w/v PEG 3350 and 0.1 M sodium citrate, pH 5.6. The crystals appeared within 24 h reaching their maximum size after 4 days. The crystals were cryoprotected using the reservoir mother liquor supplemented with 20% w/v glycerol before flash freezing in liquid nitrogen. X-ray diffraction data used for structure determination and refinement were collected at the X06SA beamline of the Swiss Light Source (SLS) in Villigen, Switzerland. Data were processed using XDS [37] and scaled with programs of the CCP4 suite [38]. Data collection and refinement statistics are listed in Supplementary Table ST1. The structure was solved with MOLREP [39], using the coordinates of rabbit skeletal muscle L-LDH (PDB: 5NQB) as search model, and refined with REFMAC5 [40]. The final coordinates were deposited in the Protein

Data Bank with accession code 7P4G. The tertiary structure representations were rendered with PyMol [41].

2.6 Analysis of LDH-A dissociation equilibria

To evaluate the dissociation of rabbit LDH-A tetramer, we assayed initial velocities of pyruvate reduction as a function of enzyme concentration, over pH values ranging from 5.0 to 7.0. Under conditions of zero-order kinetics (0.5 mM pyruvate, 125 μM β-NADH), enzyme activity was found to exponentially depend on LDH-A concentration. To interpret this, rabbit LDH-A tetramer was assumed to undergo a simple dissociation equilibrium:

$$T \overset{K_D}{\rightleftharpoons} M \qquad (1)$$

Accordingly, the total concentration of enzyme subunits can be expressed as:

$$[S_t] = \sqrt{\sqrt{K_D[T]} + 4[T]} \qquad (2)$$

For each pH considered, the discrete values of activity detected in the presence of known concentrations of total subunits (S_t) were interpreted as the output of the catalytic action exclusively exerted by LDH-A tetramer. Given a particular [S_t], the value of K_D and the fraction of enzyme tetramer were estimated by solving equation (2) expressed in implicit form. To this aim, we used the implicit equation solver in SigmaPlot to determine the best fit to the experimental observations obtained at each pH value.

2.7 Dynamic light scattering

Dynamic light scattering experiments were performed with a Malvern Panalytical (Malvern, UK) Zetasizer Nano ZS system. All the measurements were recorded at 25 °C using solutions previously

filtered with 0.2 μm filters. Scattering was evaluated at an angle of 173 degrees. Each individual observed value of enzyme diameter represents the average output of 3 groups of consecutive determinations. Raw data were analyzed with the Zetasizer software (Malvern Panalyticals), release 7.11, and the main relevant peaks accordingly identified were further inspected using the Fityk program [42]. By this means, the area of each peak was normalized to 1, and then deconvoluted into a set of Gaussian distributions, with each component interpreted as a homogeneous sub-population of the enzyme ensemble.

2.8 Mass spectrometry

To verify the identity of proteins, spots were excised from gels and underwent trypsin in-gel digestion as previously reported [43]. The resulting peptides were analyzed by LC-MS/MS using a Q-Exactive instrument (Thermo-Fisher Scientific, Waltham, MA, USA) equipped with a nano-ESI source coupled with a nano-Ultimate capillary UHPLC (Thermo-Fisher Scientific) as reported elsewhere [44]. Settings were as follows: mass accuracy window for parent ion, 10 ppm; mass accuracy window for fragment ions, 50 millimass units; fixed modification, carbamidomethylation of cysteines; variable modifications, tyrosine, serine and threonine phosphorylation, lysine acetylation, arginine methylation.

2.9 Rabbit skeletal muscle cells

Rabbit skeletal muscle cells (Lot 2430) and their growth medium (Lot 230) were obtained from Cell Applications Inc. (San Diego, CA, USA). Cells were grown in T-75 flasks at a density equal to 1-2•10^5/cm^2, using the basal medium and growth supplements recommended by the supplier. Flasks were maintained at 37 °C in a 5 % CO_2 humidified incubator. To evaluate lactate levels, cells were collected 2-4 culture cycles after thawing. The fluorescent probe BCECF (2',7'-Bis-(2-carboxyethyl)-5-(6)-carboxyfluorescein, acetoxymethyl ester) was used to determine the cytosolic pH of cells. To this aim, cells were washed twice with HBSS (pH 7.3), incubated with 5 μM BCECF for 30 minutes at

room temperature under mild shaking, and finally washed twice with HBSS (pH 7.3). Intracellular acidosis was induced by washing and incubating cells in HBSS medium (devoid of bicarbonate and supplemented with Hepes and Mes buffers, 10 mM each) at pH 6.5. Control samples were prepared with cells washed and incubated in HBSS medium at pH 7.3. The fluorescence of BCECF was determined using a Perkin-Elmer (Waltham, MA, USA) Enspire microplate reader, exciting samples at 440 or 490 nm, and evaluating emission at 535 nm. The calibration of BCECF fluorescent response to pH was obtained by exposing cells to a medium containing 0.8 mM $MgSO_4$, 1.8 mM $CaCl_2$, 140 mM KCl, 5 mM glucose, supplemented with Mes and Hepes buffers (10 mM each), and conditioned at pH values ranging from 5.0 to 8.0. After addition of 10 μM nigericin, cells were incubated for 10 minutes at room temperature under mild shaking, and the fluorescence of BCECF was finally determined under the same conditions used to estimate cytosolic pH.

2.10 Lactate assay

The concentration of lactate released by rabbit skeletal muscle cells was determined using two independent methods, relying on colorimetric [45,46] or enzymatic [47] detection. Cells ($5 \bullet 10^5$/well) were seeded in 6-well plates and let to adhere overnight. After adhesion, growth medium was replaced with 1 mL of HBSS (at pH 6.5 or 7.3) containing 20 mM glucose and cells were let to equilibrate for 3 h in a 37 °C incubator. After 3h of further incubation at 37 °C, HBSS medium was collected from each well to evaluate lactate levels. Duplicate experiments were performed. The enzymatic assay consisted in the addition of appropriate volumes of samples to a reaction mixture containing (final concentrations) 125 mM glycine, 40 mM hydrazine, 10 mM EDTA, 2.5 mM β-NAD^+, 105 nM rabbit LDH, pH 9.0. The increase in Absorbance at 340 nm related to the oxidation of lactate and the concomitant reduction of β-NAD^+ was observed for 3 h, a time interval sufficient to approximate reaction equilibrium (Supplementary Information, Figure S2). To estimate lactate

concentration in samples, a calibration curve was determined by a series of assays performed in the presence of known concentrations of sodium lactate (Supplementary Information, Figure S2).

3. RESULTS

3.1 Natural and recombinant rabbit LDH-A feature cooperative kinetics

As a first test, we assayed the activity of rabbit skeletal muscle LDH (LDH-A) at the expense of pyruvate and β-NADH, over a wide pH interval (4.5-8.0). Surprisingly, when the enzyme activity was tested under acidic conditions (pH 4.5-6.5), initial reaction velocities featured a sigmoidal dependence on pyruvate concentration (Fig.s 1A, 1B, and 1C), suggesting the occurrence of allosteric transitions in rabbit LDH-A. In particular, by fitting the Hill equation to the experimental observations obtained over the 4.5-6.5 pH interval (Fig.s 1A, 1B, and 1C) we determined Hill coefficients ranging from 1.34±0.17 to 2.11±0.22 (Fig. 2A). Conversely, at pH 7.0 or higher the enzyme obeyed Michaelis-Menten kinetics (Fig.s 1C, 1D, and 2A). It is also interesting to note that the mid-point variation of the Hill coefficient was determined at pH 6.0, suggesting that the transition to cooperative kinetics depends on electrostatic interactions half-titrated at this pH. This, in turn, suggests the engagement of histidine(s) in the allosteric transitions featured by rabbit LDH-A. Remarkably, histidines were shown to be involved in allosteric transitions of bacterial LDHs: i) the *Bifidobacterium longum* lactate dehydrogenase binds the allosteric effector fructose 1,6 bisphosphate (FBP) via electrostatic interactions engaging R173 and H188 [48,49], ii) the R173-H188 couple was also observed to be responsible for FBP binding in the *Lactobacillus casei* LDH [10]; iii) two histidines, i.e. H20 and H205, were found to stabilize the R-state of *L. casei* LDH via electrostatic interactions with D264 and E211, respectively [10].

When $K_{0.5}$, K_m, and V_{max} are considered, a significant pH-dependence was detected for K_m only: i) $K_{0.5}$ is approximately constant over pH 4.5-6.5, and K_m monotonically increases from pH 7.0 to 8.0 (Fig. 2B); ii) V_{max} does not undergo major variations over the pH interval considered (Fig. 2B). Overall, these observations are in agreement with those reported by Fritz for rabbit LDH-A [50], and confirm

the high pH-sensitivity of this enzyme under alkaline conditions. Concerning the pH dependence of allosteric transitions in rabbit LDH-A (Fig. 2A), we reasoned that a relevant control on this point could be exerted by post-translational modifications of the enzyme. We therefore investigated whether these modifications were essential or not for the allosteric transitions occurring in rabbit LDH-A. To this aim, we overexpressed in *Escherichia coli* recombinant rabbit LDH-A (hereafter denoted rLDH-A), which was conveniently purified (Supplementary Information, Figure S3) and used to perform activity assays at pH 5.0 and 8.0. When compared with the natural enzyme, rLDH-A features similar kinetic properties, i.e. undergoes allosteric transitions at pH 5.0 and obeys Michaelis-Menten kinetics at pH 8.0 (Fig. 3). It should however be noted that rLDH-A exerts a catalytic action which at pH 5.0 is lower than the activity of natural enzyme (Tab. 1). Indeed, at this pH the $K_{0.5}$ and V_{max} values determined for rLDH-A are respectively 2.5 and 0.2 times the corresponding values obtained for the natural enzyme (Tab. 1). Overall, the comparison of natural and recombinant LDH-A suggests that post-translational modifications may positively affect the activity of the enzyme at pH 5.0, independently of the cooperative kinetics observed at this pH. We therefore inspected by mass spectrometry the presence of these modifications in the natural enzyme, and we detected the acetylation of quite a number of lysines and the phosphorylation of Y239 (Tab.2).

As previously mentioned, LDH-A is considered to preferentially catalyze the reduction of pyruvate in the presence of β-NADH. Nevertheless, we investigated the occurrence, if any, of allosteric transitions when the enzyme catalyzes the oxidation of lactate. Remarkably, when the activity of natural LDH-A was assayed in the presence of lactate and NAD^+ at pH 5.0, the enzyme conformed to Michaelis-Menten kinetics, and featured a much weaker catalytic action when compared to that detected at pH 8.0 under the same conditions (Supplementary Information, Figure S4).

3.2 Intermediates of Krebs cycle and activation of rabbit LDH-A

Quite a number of years ago, Fritz reported that rabbit LDH-A undergoes allosteric transitions at pH 7.4, and identified some intermediates of the Krebs cycle as enzyme activators able to induce Michaelis-Menten kinetics [51]. Therefore, we thought it of interest to test the effect, if any, of the Krebs cycle intermediates on the activity of rabbit LDH-A at pH 5.0. At this pH the enzyme does indeed obey cooperative kinetics according to a Hill coefficient equal to 2.11±0.22 (Fig. 2A, Tab. 1), and β-NADH features a reasonable stability (Supplementary Information, Figure S5). The assays were performed under conditions of zero-order kinetics (in the presence of 0.5 mM pyruvate and 125 μM β-NADH), and supplementing the reaction mixtures with 2.5 mM of the compound to be tested. Remarkably, citrate, isocitrate and malate were found to activate the enzyme, with citrate being responsible for the most pronounced activation (Fig. 4). Moreover, cis-aconitate, α-ketoglutarate, succinate, and fumarate were found to significantly decrease, albeit at modest extents, the activity of rabbit LDH-A (Fig. 4).

3.3 Allosteric effectors of rabbit LDH-A

To test the action of citrate on LDH-A kinetics, we decided to assay enzyme activity in the presence of 2.5 mM citrate, 125 μM β-NADH, and variable concentrations of pyruvate. As expected for an allosteric activator, citrate induced the enzyme to obey Michaelis-Menten kinetics (Fig. 5A). Moreover, citrate was found to increase the $K_{0.5}$ for pyruvate from 104±11 to 292±17 μM and to increase V_{max} from 170±10 to 479±16 nM/s (Fig. 5A, Tab. 3). We also determined the enzyme kinetic parameters at pH 5.0 in the presence of 2.5 mM isocitrate or malate. Not surprisingly, isocitrate induced LDH-A to conform to Michaelis-Menten kinetics, altering both $K_{0.5}$ and V_{max} to values significantly higher than those determined for the enzyme assayed in the absence of activator (Fig. 5B, Tab. 3). When reaction mixtures were supplemented with malate, we observed cooperative

kinetics, albeit characterized by a Hill coefficient halved when compared with the coefficient obtained with assays performed in the absence of malate (Fig. 5C, Tab. 3). In addition, and as expected, the effect of malate on both $K_{0.5}$ and V_{max} was similar to that triggered by isocitrate, although according to a lower magnitude (Tab. 3).

Finally, we tested the action on rabbit LDH-A of fructose 1,6-bisphosphate (FBP), a well-known activator of allosteric LDHs [10]. Remarkably, the presence of 2.5 mM FBP in assay mixtures triggered an increase of V_{max} from 117±9 to 398±12 nM/s (Fig. 5D, Tab. 3). Moreover, hyperbolic kinetics was observed in the presence of fructose 1,6-bisphosphate (Fig. 5D).

3.4 Inhibition/activation of rabbit LDH-A by citrate

We further inspected the action exerted by citrate on rabbit LDH-A by performing activity assays in the presence of 0.5 mM pyruvate, 125 μM β-NADH, and different concentrations of citrate. Surprisingly, we did detect a significant inhibition of LDH-A at low citrate concentrations (0.1-1.0 mM), and a consistent activation at citrate concentrations ranging from 1.25 to 7.50 mM (Fig. 6A). This complicated dependence of inhibition/activation suggests the presence of multiple citrate binding sites in LDH-A. Therefore, we attempted co-crystallization of natural rabbit LDH-A and citrate under acidic pH conditions. Crystals grew in 100 mM sodium citrate at pH 5.6, which allowed to determine the rabbit LDH-A structure as a compact tetramer that resembles that of LDH from *Lactobacillus casei* in its R state (Fig. 6B). Any attempt of co-crystallization at the same pH in the presence of both citrate and NAD^+ was unproductive. Inspection of the electron density map revealed that citrate is bound to the active site (Fig. 6C). The interactions involving the citrate in the active site are the same for all the rabbit LDH-A subunits; accordingly, our analysis will be focused on the subunit A. The electron density shows that the three carboxyl groups of citrate are oriented to a subset of polar residues located in the active site. In particular, one carboxyl group is anchored to Arg168 whereas the other two are hydrogen bonded with His192 and Asn137 (Fig. 6C). Structural

comparison was also performed with the human LDH structure (PDB code *5w8i*) that was solved in the presence of citrate in the allosteric pocket (at the subunit interface, coordinated by a zinc ion) and an inhibitor in the active site that therefore hindered citrate binding [52]. Although our structure of rabbit LDH-A lacks citrate in the allosteric site, its overall conformation is highly similar to that of the human enzyme (Fig. 6D), which confirms that even under acidic conditions this corresponds to the active form of the enzyme. Accordingly, we propose that rabbit LDH-A, provided as ammonium sulphate suspension, can be isolated by gel filtration as a stable compact tetramer that is then maintained by the high protein concentration conditions necessary for crystallization. Likely, this prevents citrate to bind to the allosteric site, which can instead be hosted in the active site as inhibitor. Citrate uniquely bound to the LDH active site was previously observed only in the structure of dogfish M4 LDH at physiological pH (PDB code *8ldh*) [53]. Nevertheless, in that case the tetramer that can be reconstituted as crystallographic assembly from the monomer present in the asymmetric unit cannot be clearly interpreted as the active R form.

3.5 Dependence of rabbit LDH-A activity on enzyme concentration

The catalytic performance of rabbit LDH-A was shown to feature a peculiar dependence on enzyme concentration [54]. When the reduction of pyruvate catalyzed by rabbit LDH-A was assayed at pH 7.4 in the presence of ca. 2 µg/mL of enzyme, an activity equal to approximately 0.6 mM/s•mg was observed [54]. However, when the enzyme concentration in the assay was decreased to about 1 µg/mL, pyruvate reduction was barely detectable, and turned extremely modest, if at all, at concentrations slightly lower than 1 µg/mL [54]. These observations can be explained with the sensitivity of rabbit LDH-A to undergo dilution-induced dissociation. It was indeed reported that when the enzyme is diluted at concentrations lower than 1 mg/mL (at pH 7.0) a slow but significant dissociation occurs [55]. Moreover, it was also shown that LDH-A at 0.1 mg/mL is equally partitioned into tetramer and dimer+monomer, and that a slight further dilution to 0.05 mg/mL triggers

consistent dissociation of the tetramer, accounting for 10 % only of the total enzyme [56]. Remarkably, elegant assays were used to show that immobilized and dissociated rabbit LDH-A is able to reassemble with free subunits, although this reassociation competence is rapidly lost [57]. By reasoning that rabbit LDH-A dissociation could be greatly affected by pH, we decided to perform activity assays as a function of enzyme concentration over the 5.0-7.0 pH interval, under conditions of zero-order kinetics. Surprisingly, we were unable to detect a linear dependence of activity on enzyme concentration, even at neutral or slightly acidic pH (Fig. 7A). Moreover, a pronounced exponential dependence was instead detected at pH 5.0-6.0 (Fig. 7A). It is also interesting to note that the concentration of enzyme necessary to yield an activity equal to about 3500 nM/s is inversely related to pH (Fig. 7A). Overall, these observations can be interpreted as the output of pH-dependent dissociation equilibria of the LDH-A tetramer, with dimer and monomer featuring an extremely modest, if at all, catalytic action. To attempt a quantitative evaluation of this interpretation we used a simple model, i.e. we expressed the total concentration of subunits as the sum of monomer and tetramer concentrations, whose molar ratio is linked to tetramer-monomer dissociation constant (K_D, see Methods). Using the implicit equation solver in SigmaPlot, we calculated the K_D values yielding a satisfactory solution for the dependence of activity on enzyme concentration (at each pH considered), assuming tetramer as the unique enzyme form featuring a significant catalytic action. By this means, we obtained high K_D values occurring at pH 5.0 and 5.5 (Fig.s 7B and 7D), and a reasonable fitting to the experimental observations (Fig. 7B). Moreover, we determined with the same approach much lower values for the dissociation constant at pH 6.0-7.0 (Fig.s 7C and 7D). Nevertheless, it is noteworthy that the activity of rabbit LDH-A features a maximum at pH values (6.0-6.5, Fig. 2B) inducing a significant, albeit moderate, enzyme dissociation (Fig. 7C).

3.6 Dissociation of rabbit LDH-A as a function of pH

To further inspect the pH-dependence of rabbit LDH-A dissociation, we performed dynamic light scattering (DLS) experiments. First, we estimated the diameters corresponding, over a wide length interval, to different enzyme forms. When a 6 μM LDH-A solution at pH 7.5 was analyzed, the distribution of scattering intensities was dominated by a component featuring a diameter of approximately 10 nm (Supplementary Information, Fig. S6A). Conversely, a solution containing 6 μM enzyme at pH 5.0 contained particles of very large diameter, diagnostic of LDH-A dissociation and aggregation in multimeric forms (Supplementary Information, Fig. S6A). This difference was more pronounced when the comparison was between 1.5 μM enzyme solutions, with the sample at pH 5.0 mainly represented by aggregates featuring diameters of 200-1000 nm (Supplementary Information, Fig. S6B). However, it should be noted that the sample at pH 7.5 does also feature the presence of aggregates (Supplementary Information, Fig. S6B), indicating that even at this pH dissociation occurs in diluted enzyme solutions.

To investigate in more detail the effect of pH on LDH-A dissociation, we performed a DLS experiment using enzyme samples differing by 0.5 pH units over the 5.0-7.5 interval. In particular, we focused our attention on the peaks centered at about 10 nm (Supplementary Information, Fig. S6), and we used the software Fityk to obtain the deconvolution of these peaks into Gaussian components. Overall, we interpreted these components as the enzyme tetramer, dimer, and two distinct monomeric forms (Fig. 8, Tab. 4). Interestingly, when the occurrence of LDH-A tetrameric and dimeric forms is considered, a sharp transition was observed between pH 6.0 and 6.5. We indeed exclusively detected LDH tetramer at pH 6.5-7.5, with the enzyme ensemble dominated by dimer and monomers at pH 5.0-6.0 (Fig. 8, Tab. 4). This relation between pH and enzyme dissociation resembles the effect of pH on the LDH-A Hill coefficient, the value of which was determined as equal to 1 at pH values higher than 6.5 (Fig. 2). Accordingly, we propose that the cooperative kinetics

featured by rabbit skeletal muscle LDH-A stems from the action of pyruvate in promoting the assembly of the tetrameric enzyme under acidic conditions. In addition, we suggest that citrate, isocitrate, malate, and fructose 1,6-bisphosphate exert a similar action, opposing the enzyme dissociation induced by acidic pH values.

We further inspected and analyzed by DLS solutions containing 1.5, 3.0, or 6 μM enzyme, at pH 5.0 or 7.5. The observations obtained under these conditions suggest that: i) the size of the estimated diameters is essentially independent of enzyme dilution (Supplementary Information, Fig. S7); ii) enzyme dilution triggers moderate but significant dissociation of tetramer at pH 7.5, as revealed by the decrease of the corresponding peak area (Supplementary Information, Tab. ST2); iii) the acidic pH enhances the dilution-induced dissociation of enzyme tetramer and dimer (Supplementary Information, Tab. ST2).

To test the effect of pyruvate and citrate on enzyme dissociation, we analyzed by DLS the quaternary structure of LDH-A at pH 5.0, 6.5, and 7.5, using enzyme samples supplemented with 2.5 mM β-NAD^+ and 0.5 mM pyruvate, or with 2.5 mM citrate, to be compared with enzyme samples devoid of any additive. Remarkably, both pyruvate/β-NAD^+ and citrate were observed to counteract the dissociation of LDH-A induced by acidic pH (Supplementary Information, Tab. ST3). In particular, the presence of pyruvate/β-NAD^+ or citrate was observed to: i) allow the assembly of LDH-A tetramer at pH 6.5, with citrate being responsible for the most pronounced effect (Supplementary Information, Tab. ST3); ii) enable the generation of enzyme dimer at pH 5.0 (Supplementary Information, Tab. ST3). These observations suggest that the assembly of quaternary structures of LDH-A is responsible for the cooperative kinetics when the enzyme activity is assayed as a function of pyruvate (Fig. 1), and for the transition to Michaelis-Menten kinetics when 2.5 mM citrate is added to LDH reaction mixtures (Fig. 5A).

Finally, it is important to note that the diameters estimated for the different LDH-A association forms appear to be consistent. Indeed, by taking into account all the estimated values (Tab.s 4-6) the mean diameter for LDH-A tetramer, dimer, and for the two distinct monomers were calculated as equal to 12.95±0.83, 10.64±0.36, 8.95±0.34, and 7.46±0.52 nm, respectively.

3.7 Cytosolic pH of rabbit skeletal muscle cells and generation of lactate

As previously mentioned, the activity of rabbit LDH-A is maximal at pH 6.0-6.5 (Fig. 2B), i.e. under conditions responsible for significant enzyme dissociation. Therefore, we thought it of interest to test how the catalytic features of rabbit LDH-A *in vitro* can be related to the generation of lactate *in vivo*. To this aim, we used primary rabbit skeletal muscle cells, and we investigated the influence of an external buffered medium on the cytosolic pH. In particular, we determined the cytosolic pH (with the fluorescent probe BCECF) of cells exposed to modified HBSS medium (see Methods) buffered at pH 7.3 or 6.5. First, we calibrated the BCECF fluorescence emission ratio (490/440 nm) of cells treated with nigericin and subjected to a wide interval of pH conditions (Supplementary Information, Fig. S8). Further, by means of BCECF fluorescence we determined the cytosolic pH of cells cultured in growth medium, and then shifted to HBSS medium at pH 7.3 or 6.5, in the absence of nigericin. Not surprisingly, the cytosolic pH of cells shifted to HBSS medium at pH 7.3 did not appreciably change over a time interval of 3 h (Fig. 9A). However, the cytosolic pH of cells shifted to HBSS medium at pH 6.5 attained, after an initial fast and consistent decrease, a steady-state after 2-3 h (Fig. 9A). Therefore, we decided to assay the lactate produced by rabbit skeletal muscle cells exposed for 6 h to HBSS medium at pH 7.3 or 6.5, and we determined the lactate secreted by these cells using two independent analytical procedures (see Methods). Interestingly, and independently on the analytical method used, the level of lactate produced by cells poised to the lower pH was found to be about 3 times lower when compared with the lactate released by cells maintained at pH 7.3 (Fig. 9B). We interpret this observation as the outcome of enzyme dissociation occurring in

cells at the acidic pH, with this effect outperforming the better catalytic efficiency of the enzyme under this pH condition.

4. DISCUSSION

In contrast to their prokaryotic counterparts, eukaryotic lactate dehydrogenases are usually considered enzymes featuring Michaelis-Menten kinetics [19]. To test the occurrence of allosteric transitions in a eukaryotic enzyme, we used rabbit skeletal muscle LDH-A as a model system. It was indeed reported that this enzyme undergoes allosteric transitions [51] and features allosteric-like large-scale motions [58]. In particular, Fritz detected cooperative kinetics by performing activity assays at pH 7.4 in the presence of rabbit skeletal muscle LDH [51]. We report here on the pH-dependent nature of the allosteric transitions occurring in rabbit LDH-A, and we show that Hill coefficients ≥ 1 were exclusively determined at acidic pH values (Fig. 2). This apparent inconsistency can be accounted for by the different activity assay conditions, i.e. the lower β-NADH (22.4 μM) and enzyme concentration (0.2 nM) used by Fritz [51] when compared to our assay conditions (125 μM β-NADH and 3 nM LDH-A). These differences are most likely responsible for a higher degree of enzyme dissociation in assays performed with low enzyme concentration [56], and suggest that the allosteric nature of rabbit LDH-A is linked to the action of pyruvate in promoting the assembly of enzyme tetramer. This was tested here by activity assays carried out as a function of enzyme concentration, and by DLS experiments. In particular, at acidic pH values we observed an exponential dependence of LDH-A activity on enzyme concentration (Fig. 7), and it is important to note that this type of dependence is diagnostic of allosteric transitions linked to dissociation-reassociation of oligomeric enzymes [59,60]. In addition, our DLS experiments do directly demonstrate the pH-dependent dissociation of rabbit LDH-A tetramer, with citrate and pyruvate counteracting this dissociation.

The observation that the binding of ligands to multimeric proteins (e.g. the association of O_2 to hemoglobin) can occur according to a sigmoidal dependence on ligand concentration [61,62] led to

the proposal of two models of allostery [11,63]. These two models share the interpretation of allostery as a molecular mechanism engaging protein structural rearrangements, but differ in how protein subunits are considered to undergo a conformational change from a low- to a high-affinity state. In particular, the Monod-Wyman-Changeux [11] and Koshland-Némethy-Filmer [63] models postulate the isomerization of protein subunits via concerted and sequential processes, respectively. As an alternative to these models, the occurrence of allostery via perturbations of protein dynamics induced by ligand binding (and not necessarily implying conformational transitions) was proposed by Cooper and Dryden [64], with this view steadily gaining attention thereafter [65-66]. In addition, shortly afterwards the formulation of the MWC and KNF models, it was proposed that allostery may also arise from dissociation-association equilibria of multimeric proteins, independently of conformational rearrangements [67,68]. More recently, this way to allostery was shown to be responsible for the structural and functional reshaping of oligomeric enzymes, and is accordingly denoted as the morphein model [60]. Taking into account the different models of allostery and considering the observations reported here, we propose that the allosteric nature of rabbit LDH-A is linked to pH-dependent association-dissociation equilibria of its subunits. Interestingly on this, it was reported for *Bifidobacterium longum* LDH that the structural elements subjected to allosteric transitions are also responsible for the assembly of the tetrameric enzyme [69].

In agreement with previous evidence on the binding of citrate to human LDH-A active site at pH 5.6 [70], we identified the association of four molecules of citrate to the active sites of tetrameric rabbit LDH-A (Fig. 6D). Notably, the occurrence of this binding accounts for the significant inhibition exerted by low citrate concentrations on rabbit LDH-A activity (Fig. 6A). However, it should be noted that we did not detect any citrate bound at the interfaces of rabbit LDH-A subunits, as it would be expected when considering that citrate limits enzyme dissociation (Tab. 6). Nevertheless, the

quaternary structure of rabbit LDH-A that we obtained at pH 5.6 in the presence of 0.1 M citrate is diagnostic of a R state, i.e. of a conformation similar to that reported for active tetrameric *Lactobacillus casei* LDH, which undergoes allosteric transitions induced by anions binding at the subunits interfaces [10]. Accordingly, we propose that citrate does transiently bind a secondary (allosteric) low-affinity site of rabbit LDH-A, with this binding inducing the assembly of the enzyme into a tetrameric active R state, the establishment of which is followed by citrate dissociation. Alternatively, the high enzyme concentration necessary to attempt crystallization would lead to a citrate-independent assembly of tetrameric LDH-A, with citrate being associated to the high affinity site only (the catalytic site). It should be noted that this implies that rabbit muscle LDH would spontaneously assemble into an active R state under high concentration conditions, and that the attainment of this state by diluted enzyme solutions would rely on pH- and pyruvate-dependent allosteric transitions.

To investigate the consequences of acidic conditions on the generation of lactate *in vivo*, we used primary rabbit skeletal muscle cells exposed to HBSS medium poised at pH 7.3 or 6.5. By this means we were able to observe that the cytosolic pH of these cells did rapidly equilibrate with the external pH (Fig. 9A). Remarkably, we detected a parallel decrease of both cytosolic pH and secretion of lactate (Fig. 9), suggesting that the lower cytosolic pH induces LDH-A dissociation *in vivo*. It should indeed be considered that the maximal activity of rabbit LDH-A occurs at pH 6.5, as we showed here, in agreement with previous data reported by Fritz [50].

5. CONCLUSIONS

Overall, the observations reported here suggest a complex regulation of muscular lactic acidosis. The decrease in cytosolic pH from physiological slightly alkaline values to moderate acidic values which is concomitant to the generation of lactate elicits a dual effect on rabbit LDH-A, with the enzyme increasing its catalytic efficiency and facing significant dissociation of its tetrameric form. These effects are, in turn, regulated by the levels of pyruvate, fructose 1,6 bisphosphate, and by some intermediates of the Krebs cycle (citrate, isocitrate, and malate), eventually counteracting the dissociation of the enzyme tetramer and the decrease of LDH-A activity. The mutual interactions of these molecular factors are therefore responsible for the competence of muscles in successfully sustaining fatigue or limited oxygen availability. It is our opinion that quite a number of these interactions deserve further analysis, both *in vitro* and *in vivo*. Accordingly, we hope that our work will stimulate additional investigations on the enzymology of lactic acidosis, a challenging and appealing biochemical issue.

Funding

Financial support by CSGI is greatly acknowledged.

Data Availability

The coordinates for the rabbit LDH-A structure in complex with citrate were deposited in the RCSB PDB Data Bank (Deposition D_1292116984) and can be accessed with the 7P4G code.

Competing Interests

The authors declare that there are no competing interests associated with the manuscript

Authors Contributions

L.G.I, M.R., G.D.S., V.R., C.B., M.B., F.T., A.P.P., F.D.P., and A.H. performed the experiments. S.C. helped in interpreting dynamic light scattering data. A.H. designed the study and wrote the manuscript.

REFERENCES

[1] F.J. Carr, D. Chill, N. Maida, The lactic acid bacteria: a literature survey, Crit. Rev. Microbiol. 28 (2002) 281-370.

[2] E.I. Garvie, Bacterial lactate dehydrogenases, Microbiol. Rev. 44 (1980) 106-139.

[3] S. Kochhar, P.E. Hunziker, P. Leong-Morgenthaler, H. Hottinger, Primary structure, physicochemical properties, and chemical modification of the NAD^+-dependent D-lactate dehydrogenase, J. Biol. Chem. 267 (1992) 8499-8513.

[4] A. Razeto, S. Kochhar, H. Hottinger, M. Dauter, K.S. Wilson, V.S. Lamzin, Domain closure, substrate specificity and catalysis of D-lactate dehydrogenase from *Lactobacillus bulgaricus*, J. Mol. Biol. 318 (2002) 109-119.

[5] S. Kim, S. Gu, Y.H. Kim, K. Kim, Crystal structure and thermodynamic properties of D-lactate dehydrogenase from *Lactobacillus jensenii*, Int. J. Biol. Macromol. 68 (2014) 151-157.

[6] B. Jia, Z.J. Pu, K. Tang, X. Jia, K.H. Kim, X. Liu, C.O. Jeon, Catalytic, computational, and evolutionary analysis of the D-lactate dehydrogenases responsible for D-lactic acid production in lactic acid bacteria, J. Agr. Food Chem. 66 (2018) 8371-8381.

[7] G. Le Bras, J. Garel, Properties of D-lactate dehydrogenase from *Lactobacillus bulgaricus*: a possible different evolutionary origin for the D- and L-lactate dehydrogenases, FEMS Microbiol. Lett. 79 (1991) 89-94.

[8] N. Furukawa, A. Miyanaga, M. Togawa, M. Nakajima, H. Taguchi, Diverse allosteric and catalytic functions of tetrameric D-lactate dehydrogenases from three Gram-negative bacteria, AMB Express 4 (2014) 76.

[9] A. Steinbüchel, H.G. Schlegel, Nad-linked L(+)-lactate dehydrogenase from the strict aerobe *Alcaligenes eutrophus*, Eur. J. Biochem. 130 (1983) 321-328.

[10] K. Arai, T. Ishimitsu, S. Fushinobu, H. Uchikoba, H. Matsuzawa, H. Taguchi, Active and inactive state structures of unliganded *Lactobacillus casei* allosteric L-lactate dehydrogenase, Proteins 78 (2009) 681-694.

[11] J. Monod, J. Wyman, J. Changeux, On the nature of allosteric transitions: a plausible model, J. Mol. Biol. 12 (1965) 88-118.

[12] Y. Takenaka, G.W. Schwert, Lactic dehydrogenase: III. Mechanism of the reaction, J. Biol. Chem. 223 (1956) 157-170.

[13] G.L. Long, N.O. Kaplan, D-lactate specific pyridine nucleotide lactate dehydrogenase in animals, Science 162 (1968) 685-686.

[14] M.J. Flick, S.F. Konieczny, Identification of putative mammalian D-lactate dehydrogenase enzymes, Biochem. Biophys. Res. Comm. 295 (2002) 910-916.

[15] N.O. Kaplan, M.M. Ciotti, F.E. Stolzenbach, Reaction of pyridine nucleotide analogues with dehydrogenases, J. Biol. Chem. 221 (1956) 833-844.

[16] N.O. Kaplan, M.M. Ciotti, M. Hamolsky, R.E. Bieber, Molecular heterogeneity and evolution of enzymes, Science 131 (1960) 392-397.

[17] E. Golberg, Immunochemical specificity of lactate dehydrogenase-X, Proc. Natl. Acad. Sci. USA 68 (1971) 349-352.

[18] E.E. Montamat, N.T. Vermouth, A. Blanco, Subcellular localization of branched-chain amino acid aminotransferase and lactate dehydrogenase C_4 in rat and mouse spermatozoa, Biochem. J. 255 (1988) 1053-1056.

[19] D. Madern, Molecular evolution within the l-malate and l-lactate dehydrogenase super-family, J. Mol. Evol. 54 (2002) 825-840.

[20] C. Brochier-Armanet, D. Madern, Phylogenetics and biochemistry elucidate the evolutionary link between L-malate and L-lactate dehydrogenases and disclose an

intermediate group of sequences with mix functional properties, Biochimie 191 (2021) 140-153.

[21] W.M. Fletcher, F.G. Hopkins, Lactic acid in amphibian muscle, J. Physiol. 35 (1907) 247-309.

[22] K. Sahlin, R.C. Harris, B. Nylind, E. Hultman, Lactate content and pH in muscle samples obtained after dynamic exercise, Pflügers Arch. 367 (1976) 143-149.

[23] A. Schurr, R.S. Payne, Lactate, not pyruvate, is neuronal aerobic glycolysis end product: an *in vitro* electrophysiological study, Neuroscience 147 (2007) 613-619.

[24] G.A. Brooks, Lactate: glycolytic end product and oxidative substrate during sustained exercise in mammals – the 'lactate shuttle', in: Gilles, R. Ed., Circulation, respiration, and metabolism: current comparative approaches, Springer-Verlag, Berlin, 1985, pp. 208-218.

[25] M.J. Rogatzki, B.S. Ferguson, M.L. Goodwin, L.B. Gladden, Lactate is always the end product of glycolysis, Front. Neurosci. 9 (2015) 22.

[26] O. Warburg, On the origin of cancer cells, Science 123 (1956) 309-314.

[27] J.F. Zilva, The origin of the acidosis in hyperlactatemia, Ann. Clin. Chem. 15 (1978) 40-43.

[28] G.J. Gores, A. Nieminen, B.E. Wray, B. Herman, J.J. Lemasters, Intracellular pH during "chemical hypoxia" in cultured rat hepatocytes. Protection by intracellular acidosis against the onset of cell death, J. Clin. Invest. 83 (1989) 386-396.

[29] A. Vezzoli, M. Gussoni, F. Greco, L. Zetta, Effects of temperature and extracellular pH on metabolites: kinetics of anaerobic metabolism in resting muscle by ^{31}P- and ^{1}H-NMR spectroscopy, J. Exp. Biol. 206 (2003) 3043-3052.

[30] L.V. Thompson, E.M. Balog, R.H. Fitts, Muscle fatigue in frog semitendinosus: role of intracellular pH, Am. J. Physiol. 262 (1992) C1507-C1512.

[31] J.M. Metzger, R.H. Fitts, Role of intracellular pH in muscle fatigue, J. Appl. Physiol. 62 (1987) 1392-1397.

[32] G.B. Fiedler, A.I. Schmid, S. Goluch, K. Schewzow, E. Laistler, F. Niess, E. Unger, M. Wolzt, A. Mirzahosseini, G.J. Kemp, E. Moser, M. Meyerspeer, Skeletal muscle ATP synthesis and cellular H^+ handling measured by localized ^{31}P-MRS during exercise and recovery, Sci. Rep. 61 (2016) 32037.

[33] A.P. Pasti, V. Rossi, G. Di Stefano, M. Brigotti, A. Hochkoeppler, Human lactate dehydrogenase A undergoes allosteric transitions under pH conditions inducing the dissociation of the tetrameric enzyme, Biosci. Rep. 42 (2022) BSR20212654.

[34] C. Bernofsky, S.C. Wanda, Formation of reduced nicotinamide adenine dinucleotide peroxide, J. Biol. Chem. 257 (1982) 6809-6817.

[35] K.J. Ellis, J.F. Morrison, Buffers of constant ionic strength for studying pH-dependent processes, Methods Enzymol. 87 (1982) 405-426.

[36] M.M. Bradford, A rapid and sensitive method for the quantitation of microgram quantities of protein utilizing the principle of protein-dye binding, Anal. Biochem. 72 (1976) 248-254.

[37] W. Kabsch, XDS, Acta Cryst. D 66 (2010) 125-132.

[38] Collaborative Computational Project N. 4, The CCP_4 suite: programs for protein crystallography, Acta Cryst. D 50 (1994) 760-763.

[39] A. Vagin, A. Teplyakov, MOLREP: an Automated Program for Molecular Replacement, J. Appl. Cryst. 30 (1997) 1022-1025.

[40] G.N. Murshudov, P. Skubak, A.A. Lebedev, N.S. Pannu, R.A. Steiner, R.A. Nicholls, M.D. Winn, F. Long, A.A. Vagin, REFMAC5 for the refinement of macromolecular crystal structures, Acta Cryst. D 67 (2011) 355-367.

[41] W.L. DeLano, Use of PYMOL as a communications tool for molecular science, Abstr. Pap. Am. Chem. Soc. 228 (2004) U313-U314.

[42] M. Wojdyr, Fityk: a general-purpose peak fitting program, J. Appl. Cryst. 43 (2010) 1126-1128.

[43] A. Schevchenko, H. Thomas, J. Havliš, J.V. Olsen, M. Mann, In-gel digestion for mass spectrometric characterization of proteins and proteomes, Nat. Protoc. 1 (2007) 2856-2860.

[44] E. Conte, G. Vincelli, R.M. Schaaper, D. Bressanin, A. Stefan, F. Dal Piaz, A. Hochkoeppler, Stabilization of *the Escherichia coli* DNA polymerase III ε subunit by the θ subunit favors *in vivo* assembly of the Pol III catalytic core, Arch. Biochem. Biophys. 523 (2012) 135-143.

[45] S.B. Barker, W.H. Summerson, The colorimetric determination of lactic acid in biological material, J. Biol. Chem. 138 (1941) 535-554.

[46] F. Farabegoli, M. Vettraino, M. Manerba, L. Fiume, M. Roberti, G. Di Stefano, Galloflavin, a new lactate dehydrogenase inhibitor, induces the death of human breast cancer cells with different glycolytic attitude by affecting distinct signaling pathways, Eur. J. Pharm. Sci. 47 (2012) 729-738.

[47] P.C. Engel, J.B. Jones, Causes and elimination of erratic blanks in enzymatic metabolite assays involving the use of NAD^+ in alkaline hydrazine buffers: improved conditions for the assay of L-glutamate, L-lactate, and other metabolites, Anal. Biochem. 88 (1978) 475-484.

[48] S. Iwata, K. Kamata, S. Yoshida, T. Minowa, T. Ohta, T and R states in the crystals of bacterial L-lactate dehydrogenase reveal the mechanism for allosteric control, Nat. Struct. Mol. Biol. 1 (1994) 176-185.

[49] S. Fushinobu, K. Kamata, S. Iwata, H. Sakai, T. Ohta, H. Matsuzawa, Allosteric activation of L-lactate dehydrogenase analyzed by hybrid enzymes with effector-sensitive and -insenstive subunits, J. Biol. Chem. 271 (1996) 25611-25616.

[50] P.J. Fritz, Rabbit lactate dehydrogenase isozymes: effect of pH on activity, Science 156 (1967) 82-83.

[51] P.J. Fritz, Rabbit muscle lactate dehydrogenase 5: a regulatory enzyme, Science 150 (1965) 364-366.

[52] G. Rai, K.R. Brimacombe, B.T. Mott, D.J. Urban, X. Hu, S. Yang, T.D. Lee, D.M. Cheff, J. Kouznetsova, G.A. Benavides, K. Pohida, E.J. Kuenstner, D.K. Luci, C.M. Lukacs, D.R. Davies, D.M. Dranow, H. Zhu, G. Sulikowski, W.J. Moore, G.M. Stott, A.J. Flint, M.D. Hall, V.M. Darley-Usmar, L.M. Neckers, C.V. Dang, A.G. Waterson, A. Simeonov, A. Jadhav, D.J. Maloney, Discovery and optimization of potent, cell-active pyrazole-based inhibitors of lactate dehydrogenase (LDH), J. Med. Chem. 60 (2017) 9184-9204.

[53] C. Abad-Zapatero, J.P. Griffith, J.L. Sussman, M.G. Rossmann, Refined crystal structure of dogfish M_4 apo-lactate dehydrogenase, J. Mol. Biol. 198 (1987) 445-467.

[54] P. Bernfeld, B.J. Berkeley, R.E. Bieber, Reversible dissociation of enzymes at high dilutions and their inhibition by polyanions, Arch. Biochem. Biophys. 111 (1965) 31-38.

[55] I.C. Cho, H. Swaisgood, Factors affecting tetramer dissociation of rabbit muscle lactate dehydrogenase and reactivity of its sulfhydryl groups, Biochemistry 12 (1973) 1572-1577.

[56] S. Yamamoto, K.B. Storey, Dissociation of lactate dehydrogenase isozymes: influences on the formation of tetramers versus dimers of M4-LDH and H4-LDH, Int. J. Biochem. 20 (1988) 1261-1265.

[57] W.W.C. Chan, K. Mosbach, Effects of subunit interactions on the activity of lactate dehydrogenase studied in immobilized enzyme systems, Biochemistry 15 (1976) 4215-4222.

[58] M. Katava, M. Maccarini, G. Villain, A. Paciaroni, M. Sztucki, O. Ivanova, D. Madern, F. Sterpone, Thermal activation of ‘allosteric-like’ large-scale motions in a eukaryotic lactate dehydrogenase, Sci. Rep. 7 (2017) 41092.

[59] T.W. Traut, Dissociation of enzyme oligomers: a mechanism for allosteric regulation, Crit. Rev. Biochem. Mol. Biol. 29 (1994) 125-163.

[60] T. Selwood, E. Jaffe, Dynamic dissociating homo-oligomers and the control of protein function, Arch. Biochem. Biophys. 519 (2012) 131-143.

[61] A.V. Hill, The possible effects of the aggregation of the molecules of haemoglobin on its dissociation curves, J. Physiol. 40 (1910) iv-vii.

[62] G.S. Adair, A.V. Bock, H. Field Jr., The haemoglobin system. VI. The oxygen dissociation curve of haemoglobin, J. Biol. Chem. 63 (1925) 529-545.

[63] D.E. Koshland Jr., G. Némethy, D. Filmer, Comparison of experimental binding data and theoretical models in proteins containing subunits, Biochemistry 5 (1966) 365-385.

[64] A. Cooper, D.T.F. Dryden, Allostery without conformational change. A plausible model, Eur. Biophys. J. 11 (1984) 103-109.

[65] H.N. Mortlagh, J.O. Wrabl, J. Li, V.J. Hilser, The ensemble nature of allostery, Nature 508 (2014) 331-339.

[66] J.W. Biddle, R. Martinez-Corral, F. Wong, J. Gunawardena, Allosteric conformational ensembles have unlimited capacity for integrating information, eLife 10 (2021) e65498.

[67] L.W. Nichol, W.J.H. Jackson, D.J. Winzor, A theoretical study of the binding of small molecules to a polymerizing protein system. A model for allosteric effects, Biochemistry 6 (1967) 2449-2456.

[68] C. Frieden, Treatment of enzyme kinetic data. II. The multisite case: comparison of allosteric models and a possible new mechanism, J. Biol. Chem. 242 (1967) 4045-4052.

[69] J. Chen, D. Thirumalai, Interface residues that drive allosteric transitions also control the assembly of L-lactate dehydrogenase, J. Phys. Chem. B 122 (2018) 11195-11205.

[70] R.A. Ward, C. Brassington, A.L. Breeze, A. Caputo, S. Critchlow, G. Davies, L. Goodwin, G. Hassall, R. Greenwood, G.A. Holdgate, M. Mrosek, R.A. Norman, S. Pearson, J. Tart, J.A. Tucker, M. Vogtherr, D. Whittaker, J. Wingfield, J. Winter, K. Hudson, Design and synthesis of novel lactate dehydrogenase A inhibitors by fragment-based lead generation, J. Med. Chem. 55 (2012) 3285-3306.

	Natural LDH-A			Recombinant LDH-A		
	K_m, $K_{0.5}$ (μM)	V_{max} (nM/s)	Hill	K_m, $K_{0.5}$ (μM)	V_{max} (nM/s)	Hill
pH 5.0	64±3	120±4	2.11±0.22	164±16	24±2	2.55±0.44
pH 8.0	620±102	140±13		1075±163	187±22	

Table 1. Kinetic parameters of natural and recombinant skeletal muscle rabbit lactate dehydrogenase.

The Michaelis-Menten or the Hill equation was fitted to the experimental observations shown in Fig. 1 and in Fig. 3. Assays were performed in the presence of 3 and 2.5 nM of natural and recombinant enzyme, respectively (tetramer concentration, corresponding to 12 and 10 nM of subunits). The errors represent the standard deviations associated with the fittings.

Peptide	Modification	Observed M_r (Da)	Theoretical M_r (Da)
77-90	Acetyl-K81	1467.7492	1467.7571
119-132	Acetyl-K126	1836.9007	1836.8998
229-245	Acetyl K232 Acetyl-K243, Phospho-Y239	2106.0707	2106.0762
318-328	Acetyl-K318	1287.6696	1287.6603

Table 2. Identification of post-translational modifications of rabbit LDH-A.

Modified amino acids were identified by mass spectrometry of peptides obtained by in-gel tryptic digestion.

$K_{0.5}$ (μM)	V_{max} (nM/s)	Hill	$K_{0.5}$ (K_m) (μM)	V_{max} (nM/s)	Hill
Control[a]			**Citrate[a]**		
104±11	170±10	1.89±0.28	292±17	479±16	-
Control[b]			**Isocitrate[b]**		
78±4	233±8	3.03±0.47	107±12	696±32	-
			Malate[b]		
			94±9	440±22	1.58±0.18
Control[a]			**Fructose 1,6-bisphosphate[a]**		
118±14	117±9	2.12±0.38	71±7	398±12	-

Table 3. Effect of citrate, isocitrate, malate, and fructose 1,6-bisphosphate on rabbit LDH-A kinetic parameters.

Kinetic parameters determined from activity assays performed as a function of pyruvate concentration with rabbit LDH-A at pH 5.0 in the presence of 125 μM β-NADH (see Fig. 5). The final enzyme concentration in the assays was equal to: **a**) 2.5 nM holoenzyme (10 nM subunits); **b**) 3.5 nM holoenzyme (14 nM subunits). The same control was used to test the effect of isocitrate and malate on rabbit LDH-A activity. The errors represent the standard deviations associated with fittings of the Hill or the MIchaelis-Menten equation to the experimental observations.

Sample	Diameter (nm)	Area (%)
pH 7.5 9 µM LDH (Holo)	13.99 (T)	44.9
	12.14 (T)	34.0
	10.75 (D)	16.5
	9.72 (M1)	4.7
pH 7.0 9 µM LDH (Holo)	12.82 (T)	13.1
	10.99 (D)	14.2
	8.97 (M1)	68.6
	7.70 (M2)	4.1
pH 6.5 9 µM LDH (Holo)	12.61 (T)	9.7
	10.90 (D)	19.5
	8.72 (M1)	65. 6
	6.82 M2)	5.1
pH 6.0 9 µM LDH (Holo)	9.88 (D)	26.8
	8.99 (M1)	70.5
	8.22 (M2)	2.8
pH 5.5 9 µM LDH (Holo)	9.59 (M1)	71.8
	8.34 (M2)	28.2
pH 5.0 9 µM LDH (Holo)	9.95 (D)	56.3
	8.36 (M1)	33.4
	7.15 (M2)	10.2

Table 4. Diameters of rabbit LDH-A association forms estimated by DLS experiments.

The diameters of different rabbit LDH-A oligomers were estimated by deconvolution of the peaks observed with dynamic light scattering experiments in the presence of 9 µM enzyme (36 nM subunits), at pH values ranging from 5.0 to 7.5. In addition to the estimated diameters, the area of each component is also indicated. The area of each peak to be deconvoluted was normalized to 1. T, D, and M indicate the assignment of a detected component to enzyme tetramer, dimer, and monomer, respectively.

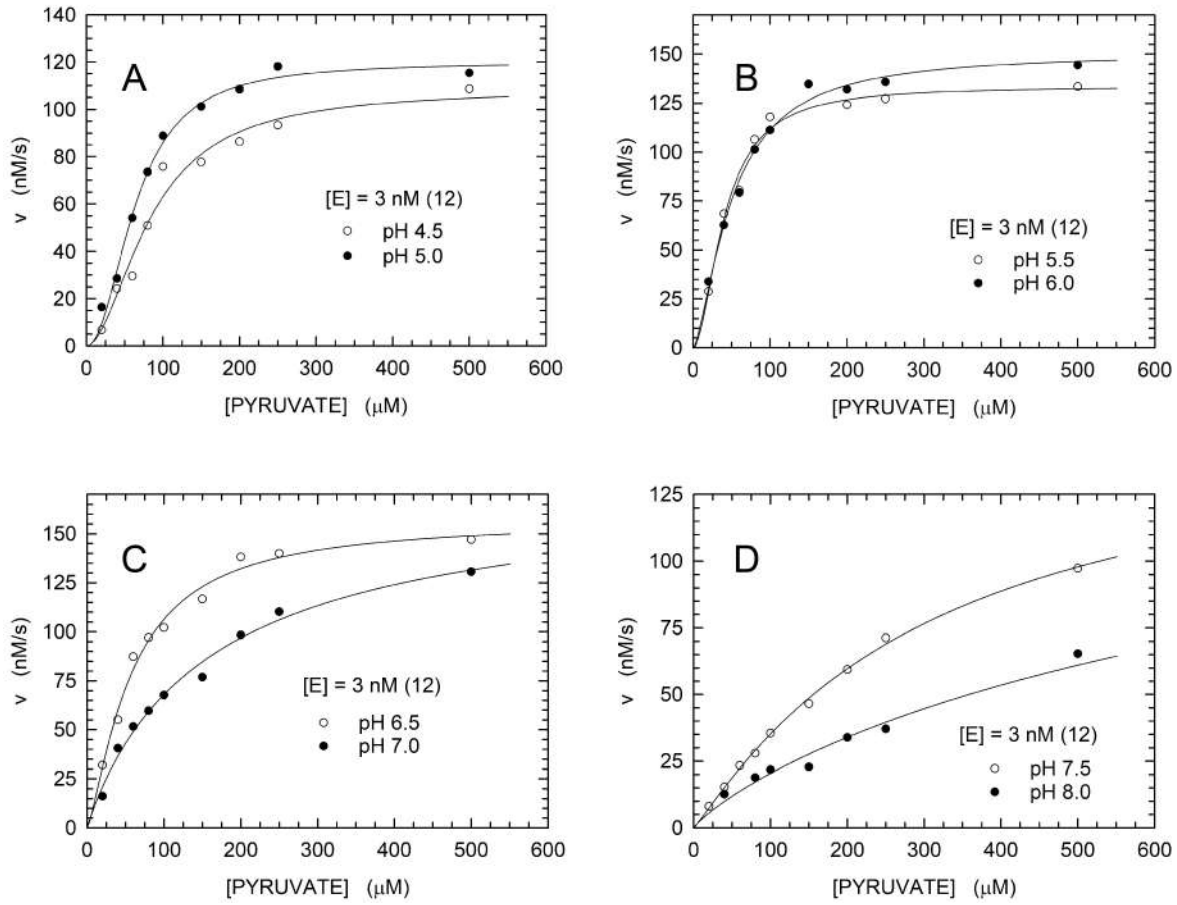

Figure 1. Kinetics of pyruvate reduction catalysed by natural rabbit LDH-A.
(A-D) Initial reaction velocities were assayed over a pH interval ranging from 4.5 to 8.0, in the presence of 3 nM LDH-A tetramer (12 nM subunits), 125 μM β-NADH, and a universal buffer (containing Mes, Mops, and Tris, 25 mM each). The dependence of initial reaction velocities on pyruvate concentration at pH 4.5 and 5.0 (A, empty and filled circles, respectively), pH 5.5 and 6.0 (B, empty and filled circles, respectively), pH 6.5 and 7.0 (C, empty and filled circles, respectively), pH 7.5 and 8.0 (D, empty and filled circles, respectively) are shown. The continuous lines represent the best fit of the Hill (pH 4.5-6.5) or the Michaelis-Menten (pH 7.0-8.0) equation to the experimental observations.

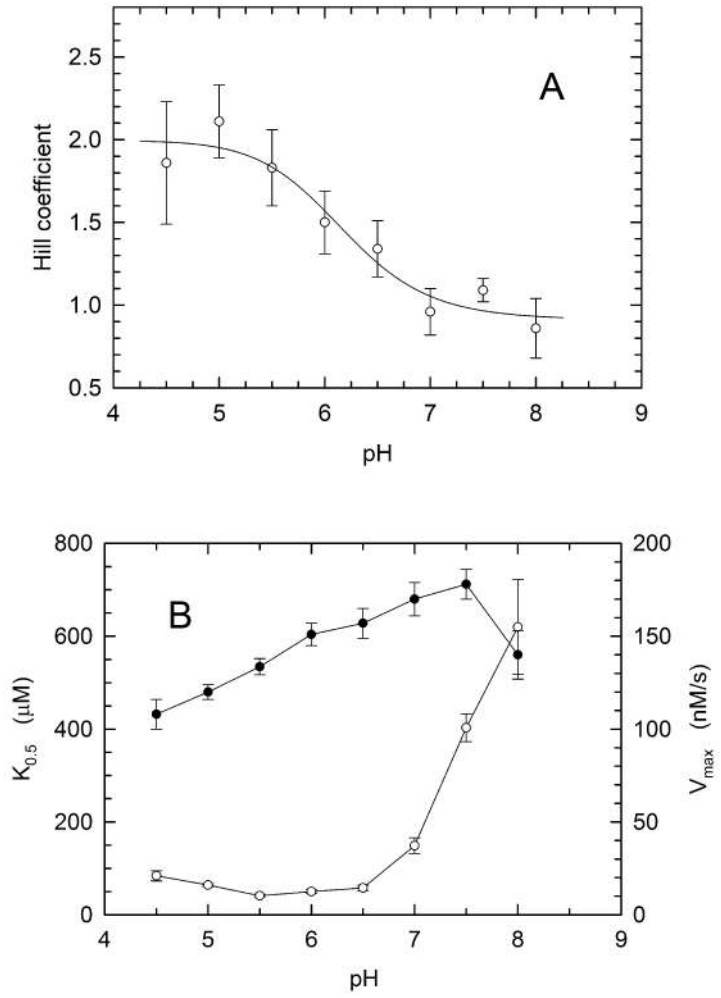

Figure 2. Kinetic parameters of natural rabbit LDH-A as a function of pH.
The values of Hill coefficient (A), $K_{0.5}$ (empty circles, B) and V_{max} (filled circles, B) were determined with the fittings shown in Figure 1 and are reported as a function of pH. In addition, the Hill coefficients at pH 7.0-8.0 were determined by fitting the Hill equation to the experimental observations.

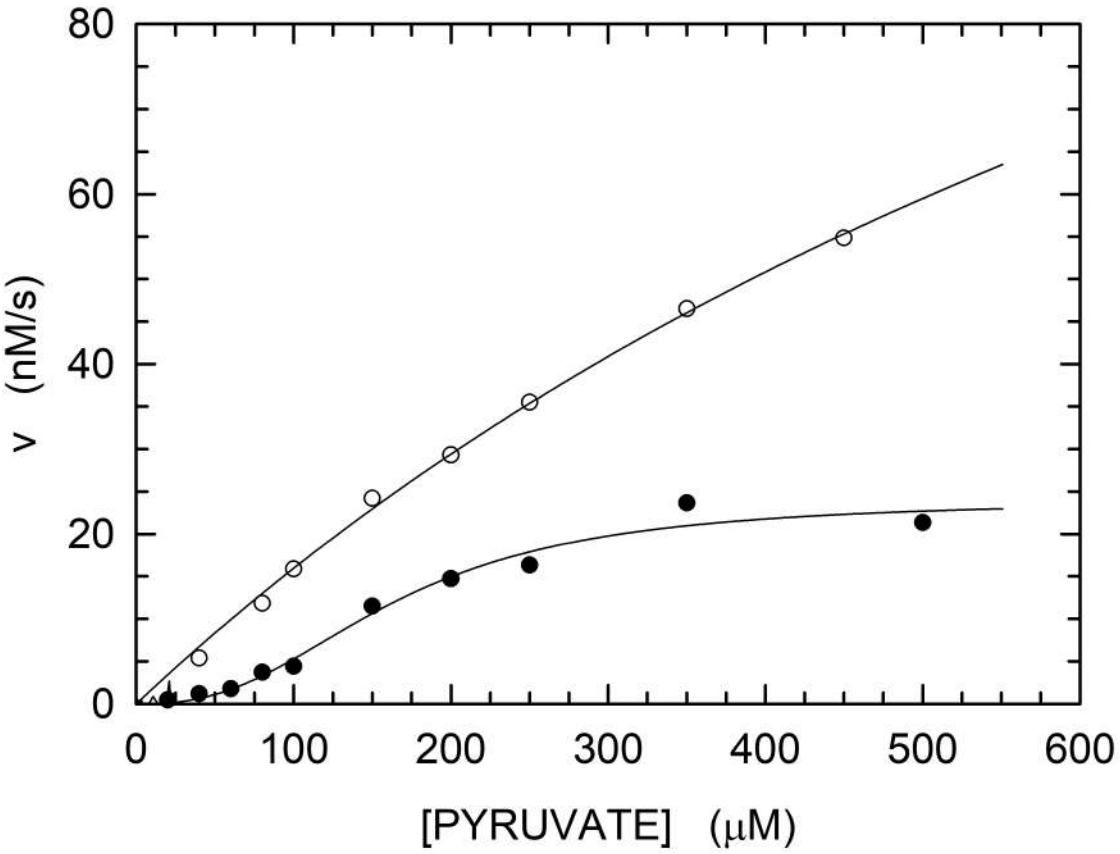

Figure 3. Kinetics of pyruvate reduction catalysed by recombinant LDH-A.
Initial reaction velocities were assayed at pH 5.0 (filled circles) and 8.0 (empty circles), in the presence of 2.5 nM LDH-A tetramer (10 nM subunits), 125 μM β-NADH, and a universal buffer (containing Mes, Mops, and Tris, 25 mM each). The continuous lines represent the best fit of the Hill (pH 5.0) or the Michaelis-Menten (pH 8.0) equation to the experimental observations.

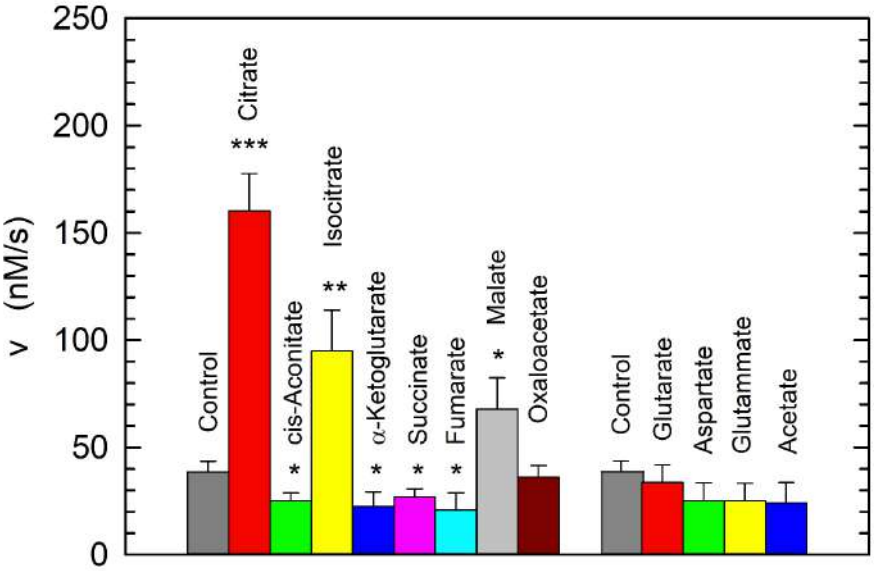

Figure 4. Effect of the Krebs cycle intermediates on the activity of natural rabbit LDH-A at pH 5.0. Initial reaction velocity was determined at pH 5.0 in the presence of 2.5 nM rabbit LDH-A tetramer (10 nM subunits), 125 µM β-NADH, and 500 µM pyruvate (control, grey bars). The LDH-A activities observed using reaction mixtures supplemented with the indicated compounds at 2.5 mM are also shown. The error bars represent standard deviation (n = 3). Experimental mean values were compared by Student's *t*-test (***, ** and * indicate P<0.001, P<0.01, P<0.05, respectively).

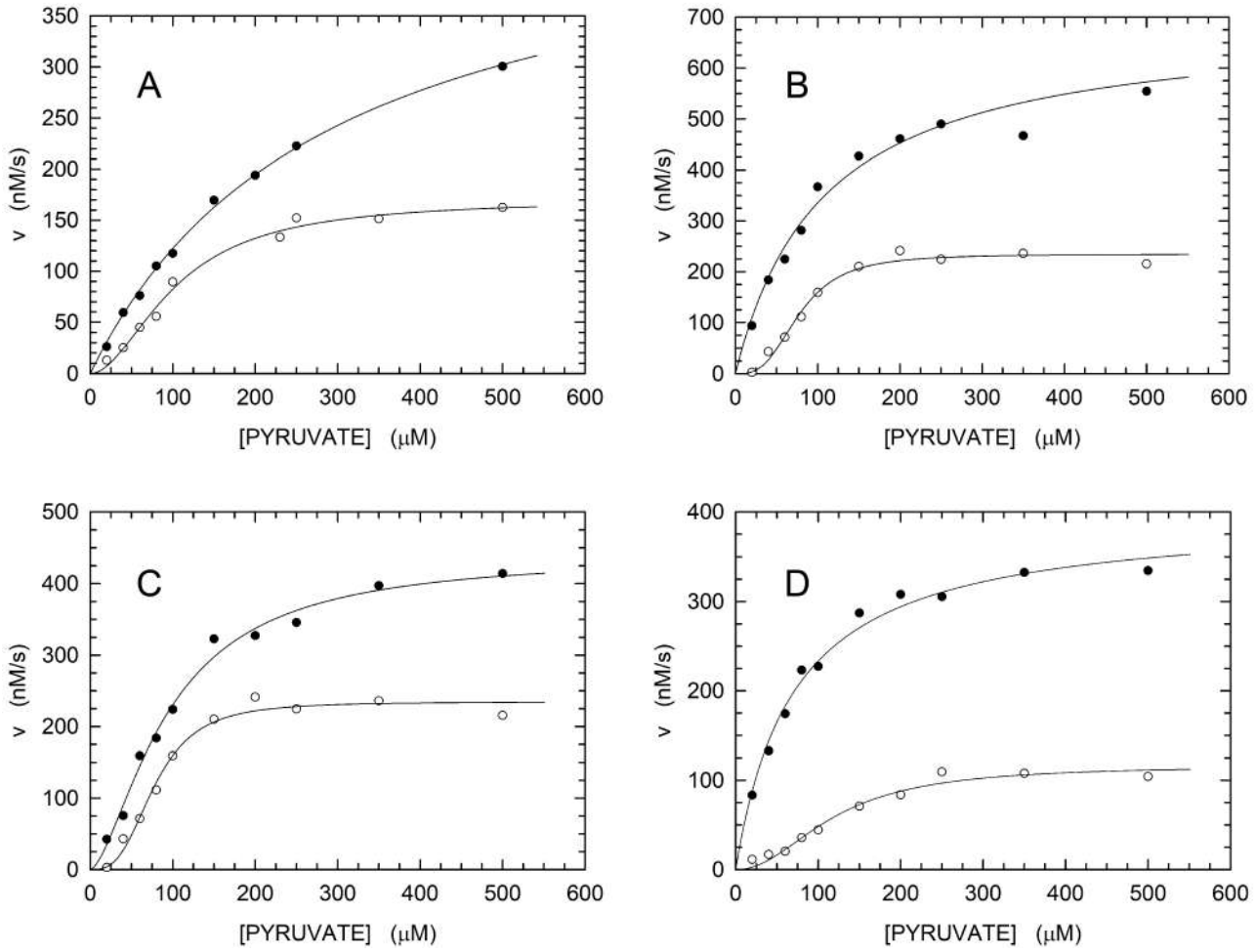

Figure 5. Kinetics of pyruvate reduction catalysed by natural rabbit LDH-A at pH 5.0.
(A) Initial reaction velocities were assayed in the presence of 2.5 nM LDH-A tetramer (10 nM subunits), 125 μM β-NADH, and a universal buffer (containing Mes, Mops, and Tris, 25 mM each). Assays were performed in the absence (empty circles) or in the presence (filled circles) of 2.5 mM citrate. The continuous lines represent the best fit of the Hill or the Michaelis-Menten equation to the experimental observations (empty and filled circles, respectively). (B) Initial reaction velocities were assayed in the presence of 3.5 nM LDH-A tetramer (14 nM subunits). Assays were performed in the absence (empty circles) or in the presence (filled circles) of 2.5 mM isocitrate. Other conditions as in Fig. 5A. The continuous lines represent the best fit of the Hill or the Michaelis-Menten equation to the experimental observations (empty and filled circles, respectively). (C) Initial reaction velocities were assayed in the presence of 3.5 nM LDH-A tetramer (14 nM subunits). Assays were performed in the absence (empty circles, same data of Fig. 5B) or in the presence (filled circles) of 2.5 mM malate. Other conditions as in Fig. 5A. The continuous lines represent the best fit of the Hill equation to the experimental observations. (D) Initial reaction velocities were assayed in the presence of 2.5 nM LDH-A tetramer (10 nM subunits). Assays were performed in the absence (empty circles) or in the presence (filled circles) of 2.5 mM fructose 1,6-bisphosphate. Other conditions as in Fig. 5A. The continuous lines represent the best fit of the Hill or the Michaelis-Menten equation to the experimental observations (empty and filled circles, respectively).

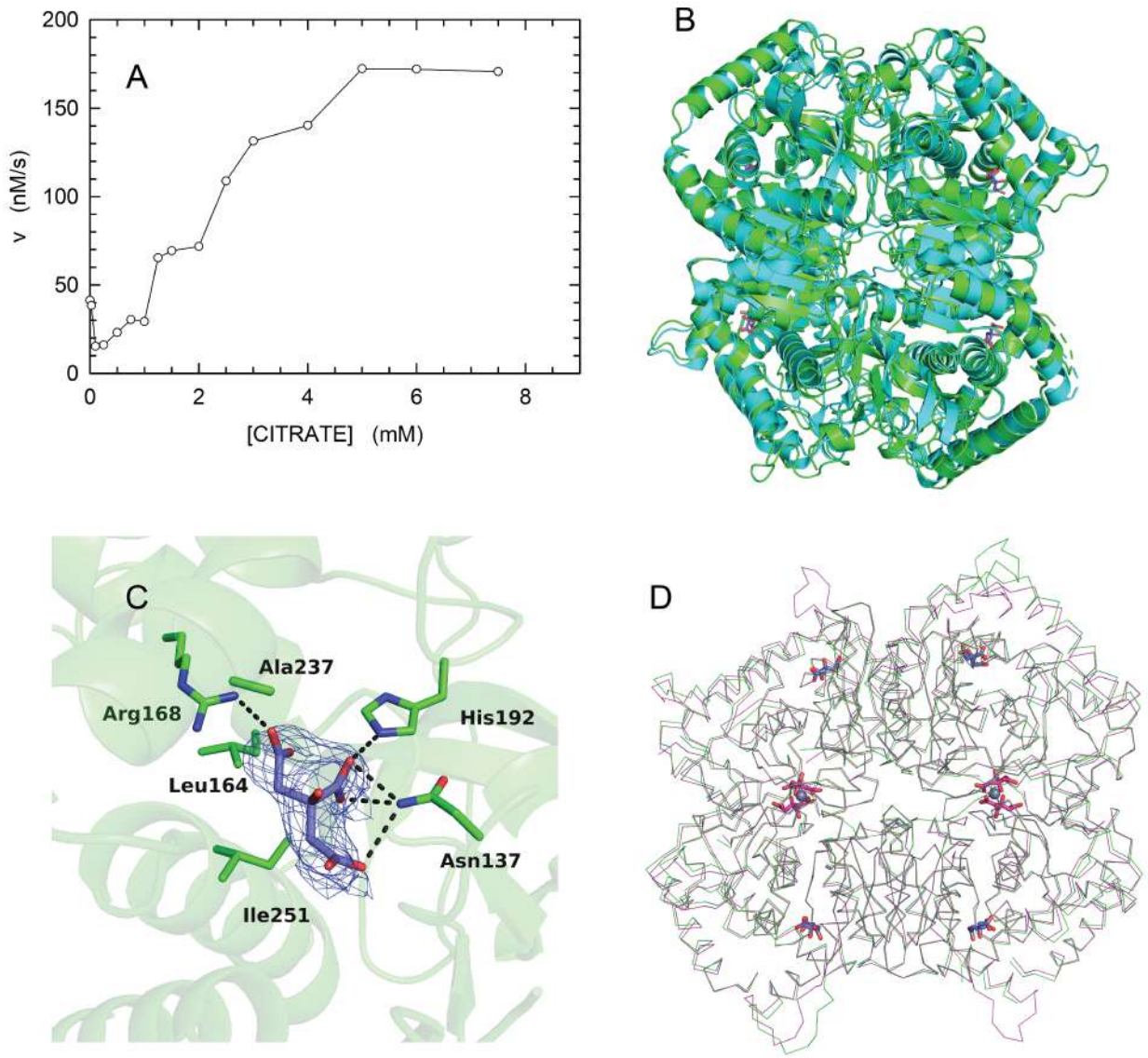

Figure 6. Citrate action on rabbit LDH-A and citrate binding sites.
(A) Activity of rabbit LDH-A as a function of citrate concentration. The assays were performed at pH 5.0 in the presence of 2.5 nM LDH-A tetramer (10 nM subunits), 125 µM β-NADH, and 500 µM pyruvate. (B) Ribbon diagram of rabbit LDH-A tetrameric structure under acidic conditions (green) superimposed on the structure of allosteric LDH from *Lactobacillus casei* in its R-state (cyan; PDB code *2zqz*). Citrate bound to each of the four subunits of rabbit LDH-A is drawn as sticks with carbon and oxygen atoms in indigo and red, respectively. (C) Zoomed view of citrate bound to rabbit LDH-A active site (protein residues with carbon, nitrogen and oxygen atoms in green, blue and red, respectively). Weighted 2Fo-Fc electron density contoured at 1.4 σ is showed for the ligand. Side chains involved in hydrogen bonding and electrostatic interactions are drawn as dashed lines. Arg168, His192 and Asn137 are anchored to the three carboxyl groups of the citrate. (D) Cα trace of the rabbit LDH-A tetramer (green) with citrate in the active site (indigo carbons) superimposed onto human LDH-A (purple) with citrate bound in the allosteric site (purple carbons) and an inhibitor occupying the active site (not shown). In the human enzyme, each pair of citrates at the subunit interface are coordinated with two zinc atoms (grey spheres).

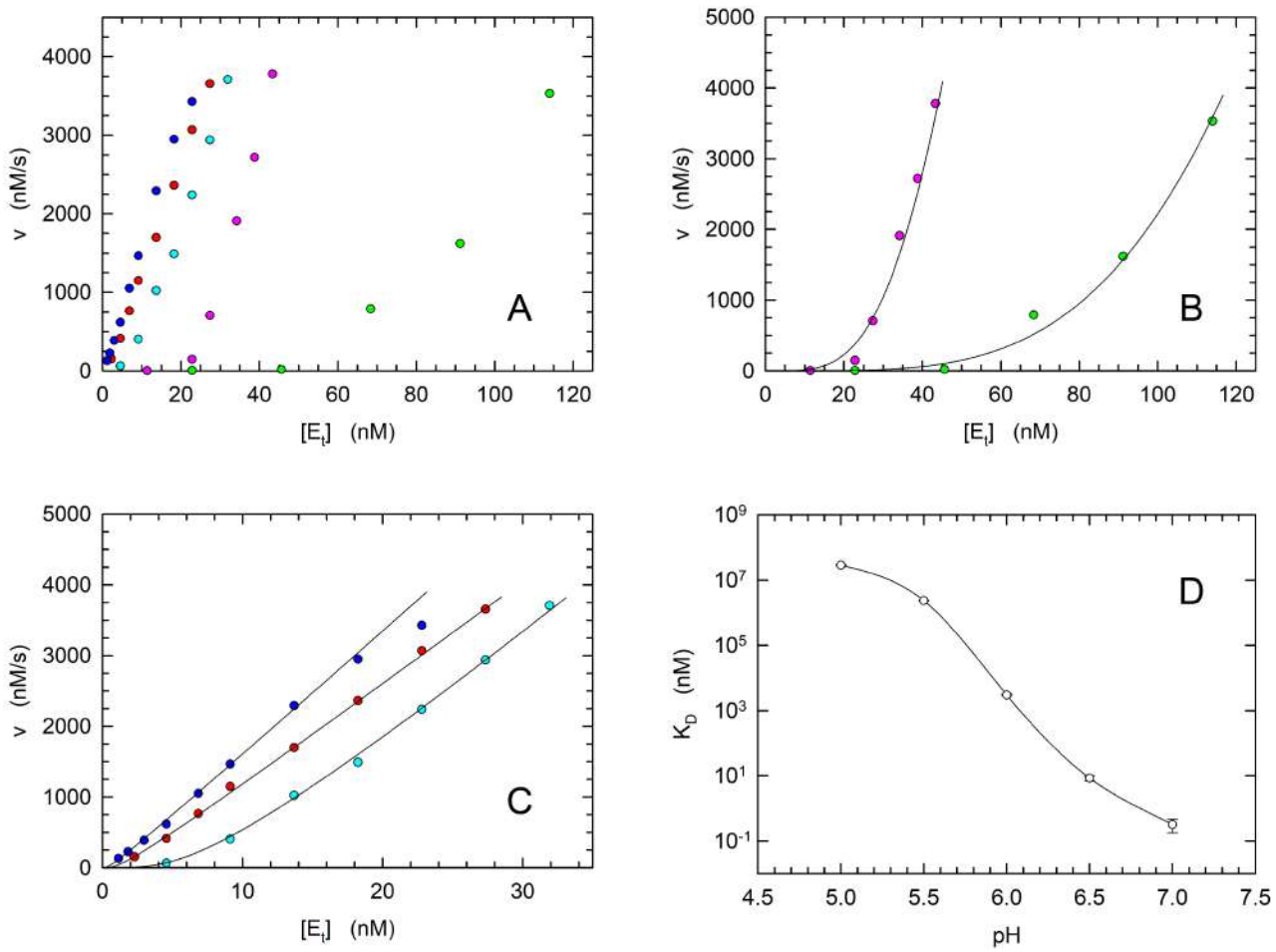

Figure 7. Activity of rabbit LDH-A as a function of enzyme concentration and pH.
(A) The activity of LDH-A was determined at pH 5.0, 5.5, 6.0, 6.5, and 7.0 (green, pink, cyan, red, and blue circles, respectively). Assays were performed in the presence of 125 µM β-NADH, and 500 µM pyruvate. Enzyme concentrations are expressed as the total concentration of subunits per assay. (B) Detail of the activity determinations performed at pH 5.0 and 5.5. The continuous lines represent the expected values of activity according to the estimations of K_D obtained with the implicit equation solver in SigmaPlot (see Methods). (C). Detail of the activity determinations performed at pH 6.0, 6.5, and 7.0. The continuous lines represent the expected values of activity according to the estimations of K_D obtained with the implicit equation solver in SigmaPlot (see Methods). (D) Dependence of K_D on pH.

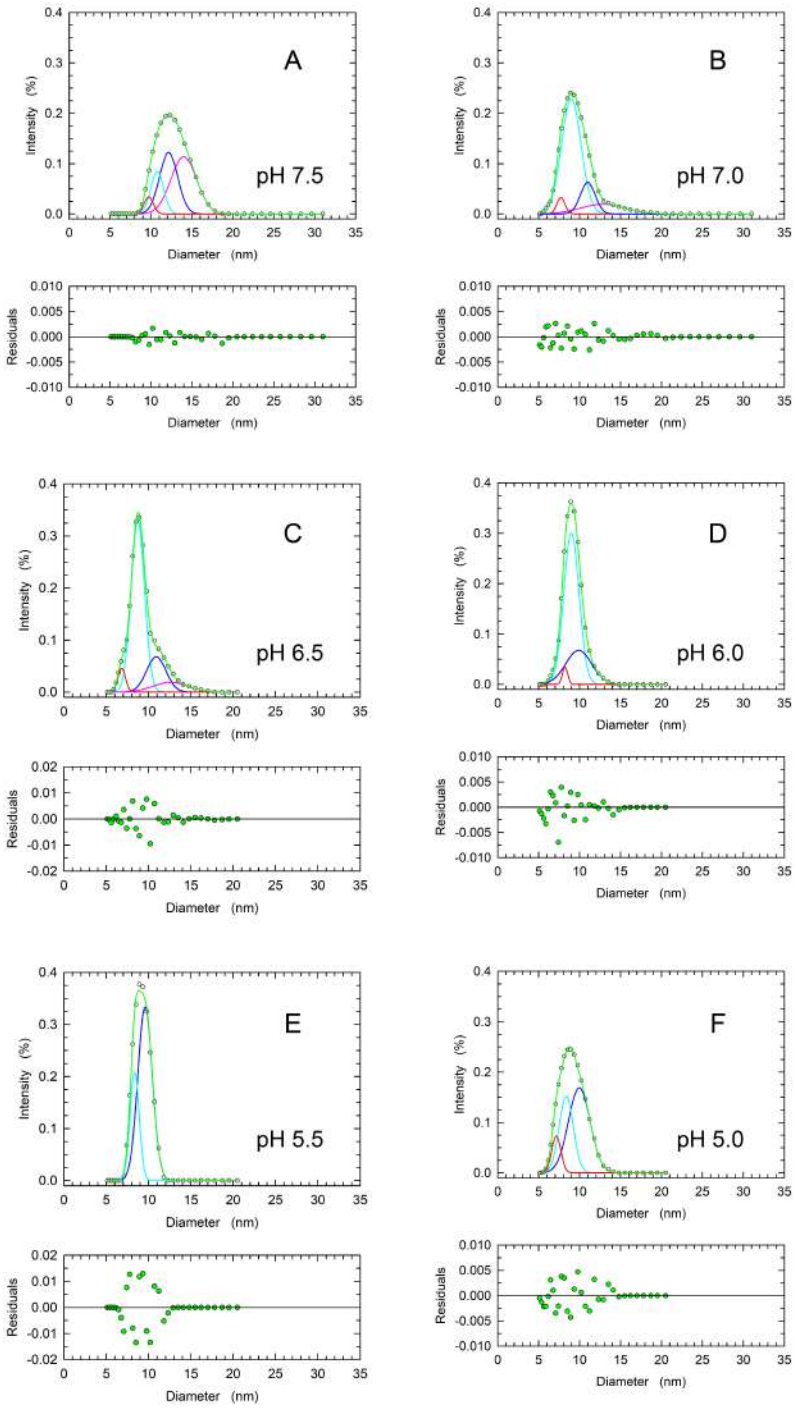

Figure 8. Association forms of rabbit LDH-A detected by dynamic light scattering as a function of pH.

(A-F) Dynamic light scattering measurements were performed in the presence of 9 µM rabbit LDH-A (36 nM subunits) as a funciont of pH. The distribution of the observed scattered intensities (empty circles) were deconvoluted with the Fityk software into an ensemble of Gaussian components (pink, blue, cyan, and red lines). The areas of the peaks to be deconvoluted were normalized to 1. The fittings to the experimental observations accordingly obtained are reported with green lines.

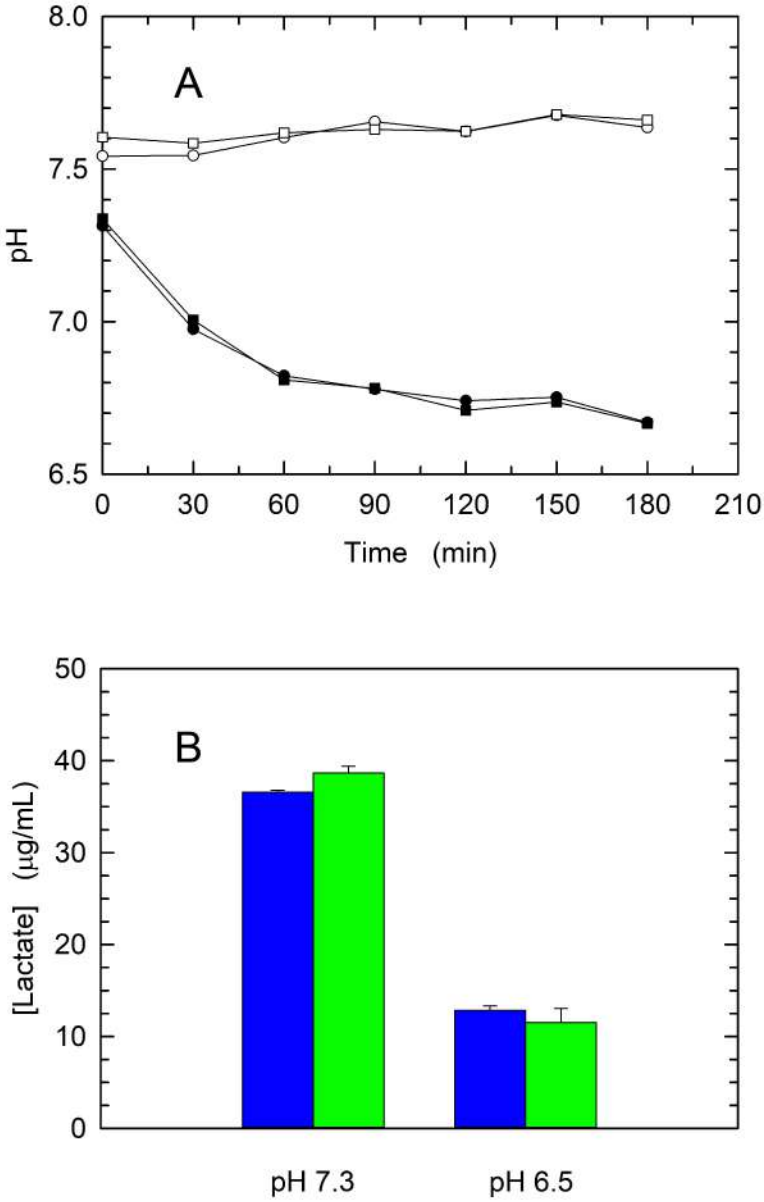

Figure 9. Cytosolic pH of rabbit skeletal muscle cells and generation of lactate.
(A) Cytosolic pH of rabbit skeletal muscle cells after their transfer from HBSS medium at pH 7.3 to the same medium (empty symbols) or to HBSS buffered at pH 6.5 (filled symbols). The values of cytosolic pH were determined using the fluorescent probe BCECF (see Methods and Supplementary Figure S8). Experiments were performed in duplicate (circles and squares). (B) Concentration of the lactate released by cells after 6 h of residence in HBSS medium at pH 7.3 or 6.5. Lactate was determined with a colorimetric (blue bars) or with an enzymatic (green bars) analytical procedure. Error bars represent the standard deviation.